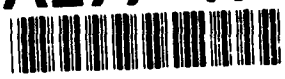

OFFICE OF NAVAL RESEARCH

GRANT: N00014-89-J-1178

TECHNICAL REPORT NO. 61

R&T CODE: 413Q001-05

ELECTRON CYCLOTRON RESONANCE PLASMA OXIDATION STUDIES OF InP

BY

Y.Z. HU, J. JOSEPH, E.A. IRENE

DEPARTMENT OF CHEMISTRY
CB#3290 VENABLE
UNIVERISTY OF NORTH CAROLINA
CHAPEL HILL, NC 27599-3290

SUBMITTED TO:

JOURNAL OF VACUUM SCIENCE AND TECHNOLOGY B

REPORT DOCUMENTATION PAGE

Form Approved
OMB No. 0704-0188

1. AGENCY USE ONLY (Leave blank)	2. REPORT DATE	3. REPORT TYPE AND DATES COVERED
	March 15, 1994	Technical Report #61

4. TITLE AND SUBTITLE
Electron Cyclotron Resonance Plasma Oxidation Studies of InP

5. FUNDING NUMBERS
N00014-89-J-1178

6. AUTHOR(S)
Y.Z. Hu, J. Joseph, E.A. Irene

7. PERFORMING ORGANIZATION NAME(S) AND ADDRESS(ES)
Department of Chemistry
University of North Carolina
CB #3290 Venable & Kenan Labs
Chapel Hill, NC 27599-3290

8. PERFORMING ORGANIZATION REPORT NUMBER
N00014-89-J-1178
Technical Report #61

9. SPONSORING/MONITORING AGENCY NAME(S) AND ADDRESS(ES)
Department of Navy
Office of Navy Research
800 North Quincy Street
Arlington, VA 22217-5000

10. SPONSORING/MONITORING AGENCY REPORT NUMBER

11. SUPPLEMENTARY NOTES
Submitted to Journal of Vacuum Science and Technology B

12a. DISTRIBUTION/AVAILABILITY STATEMENT
Reproduction in whole or in part is permitted for any purpose of the United States Government. This document has been approved for public release and sale; its distribution is unlimited.

12b. DISTRIBUTION CODE

13. ABSTRACT *(Maximum 200 words)*

Electron cyclotron resonance plasma oxidation of InP was studied using both spectroscopic and single wavelength ellipsometry employed during the oxidation process. A two layer oxide was observed with the outer layer being In rich and the inner layer P rich as confirmed from x-ray photoelectron spectroscopy and etch rate studies. Optical models and oxidation kinetics are analyzed. From positive substrate bias effects on oxidation rates, negative ion oxidant species were identified as dominant and oxide etching was observed at negative bias.

14. SUBJECT TERMS	15. NUMBER OF PAGES
Electron, cyclotron, InP, ellipsometry	16. PRICE CODE

17. SECURITY CLASSIFICATION OF REPORT	18. SECURITY CLASSIFICATION OF THIS PAGE	19. SECURITY CLASSIFICATION OF ABSTRACT	20. LIMITATION OF ABSTRACT
Unclassified	Unclassified	Unclassified	

Electron Cyclotron Resonance Plasma Oxidation Studies of InP

by
Y.Z. Hu, J. Joseph, E.A. Irene
Department of Chemistry CB# 3290
University of North Carolina
Chapel Hill, NC 27599-3290

Abstract

Electron cyclotron resonance plasma oxidation of InP was studied using both spectroscopic and single wavelength ellipsometry employed during the oxidation process. A two layer oxide was observed with the outer layer being In rich and the inner layer P rich as confirmed from x-ray photoelectron spectroscopy and etch rate studies. Optical models and oxidation kinetics are analyzed. From positive substrate bias effects on oxidation rates, negative ion oxidant species were identified as dominant and oxide etching was observed at negative bias.

Introduction

An electrically passivated semiconductor results from the oxidation of Si[1], viz. a semiconductor surface with surface state densities substantially smaller than the number of electronic carriers used for device operation. It would be desirable to be able to similarly passivate III-V semiconductor surfaces so as to take advantage of the superior semiconductor properties (carrier densities, mobilities, direct gap, etc)[2]. However, for compound semiconductors the chemical and physical interactions that occur during film forming and surface cleaning procedures often give rise to damage and altered stoichiometry that degrade the interfacial electronics properties. MOS structures with good electronics properties have been made on InP surfaces using electrochemical oxidation[3] where a passivating oxide is made under mild conditions thereby preserving the semiconductor stoichiometry. Most attempts using standard thermal oxidation techniques result in non-stoichiometric oxides, multiple inhomogeneous films, and altered stoichiometry at the InP surface[4,5] that lead to impurity related surface states. However a recent report[6] showed that electron cyclotron resonance (ECR) plasma oxidation of InP using a shutter between plasma and sample yielded an electronically good interface. It is the purpose of the present research to study the growth of oxide films on InP using the mild low temperature process afforded by ECR plasma techniques. It is known that ECR techniques produce good quality oxides on Si[7] with about the same level of interface damage as from thermal oxidation[8,9,10]. In-situ ellipsometry techniques are employed to follow the ECR oxidation of InP using both spectroscopic ellipsometry, SE, to obtain

information relative to establishing a useful and correct optical model for the oxidation, and in real time using single wavelength ellipsometry, SWE, at a carefully selected wavelength, in order to obtain film formation kinetics. X-ray photoelectron spectroscopy, XPS, was used to verify the chemical nature of the formed oxide films.

Experimental Procedures

Apparatus. The ECR system and mating in-situ rotating analyzer ellipsometer were home built and both were described previously[8,9,11] with regard to design, operation, and ellipsometer calibration. The measurement of plasma parameters has also already been discussed in some detail[12]. Background pressure of 10^{-7} torr was achievable and during oxidation, the chamber pressure was $1x10^{-3}$ torr with an O_2 flow rate of 20 sccm. The ECR plasma was operated at 2.45 GHz with 300W input microwave power. The sample was 20cm from the microwave cavity and heated with a halogen light bulb heater behind the sample, and the sample temperature was measured with a thermocouple affixed to the substrate holder. The sample holder has three translational degrees of freedom and can rotate. An O-ring sealed optical window design[11] enabled polarization free windows under all vacuum conditions. Samples could be loaded through a load lock.

Substrate Cleaning. Prior to processing, it is usually necessary to prepare or clean semiconductor substrates, in order to achieve the best electrical interfaces. Evidence exists that this step alters the InP surface[13] thus in the present work we also examine the

cleaning step. In the case of Si, it is known that the specific nature of the cleaning procedure can alter the oxidation kinetics[14,15]. In this connection Aspnes[16] has shown that the interband peaks in the ϵ_2 spectrum are particularly sensitive to semiconductor surface condition, and that a maximum value for the peaks indicates the best condition in terms of a clean surface. Figure 1 shows ϵ spectra taken on InP wafers from two sources labelled X and Y and cleaned according to our two step procedure that gives reproducible surfaces (1. A degreasing 5 min dip in each of trichloroethylene, methanol, and flowing deionized water; 2. etching for 20 s in HF(48%):MeOH = 1:40 followed by a MeOH rinse for 2 min). In a future publication we will emphasize the processes that yield the best electronic characteristics, but for our present purposes we obtain the best surfaces, in terms of the closest correspondence of ϵ_2 to the InP literature value[17], using the above cleaning procedure and the X samples. Table I contains the data from Figure 1 analyzed using a single film two component model. The two components are assumed to be a-InP and $In(PO_3)_3$. This choice is justified by the availability of dielectric function data and the goodness of fit, and the merits are discussed in the section on optical models. The figure of merit for the fit of the data to the model is the unbiased estimator, δ, defined below and shown in Table I. All three samples yield a small δ and a comparable excellent fit to the model. Atomic force microscopy, AFM was used to survey the surface roughness. For all samples the same tip and scanning parameters were used. It is seen in the table that the smallest oxide overlayer and least surface roughness results from the cleaning procedure described above on the X InP samples. Also, the cleaning procedure that we used did not measurably affect the initial surface roughness. Thus for InP it is clear that not only must

the cleaning procedure be evaluated but the initial substrate condition can vary appreciably. The SE data shows differences due to both roughness and overlayer differences that at the present time appear to be indistinguishable.

Ellipsometry Procedures. Two ellipsometry techniques were used: SE and SWE. In order to scan a spectrum of several eV, typically more than 10 minutes are required. During this time of SE data collection the plasma is stopped. Furthermore, for the oxides grown above room temperature, the samples were cooled to room temperature for SE analysis. This was done due to the temperature sensitivity of the optical properties and the unavailability of the necessary high temperature data for analysis. At each wavelength a Fourier analysis of the periodic output signal from the rotating analyzer yielded the ellipsometric parameters Δ and Ψ from which the complex reflection coefficient ρ_{exp} is obtained:

$$\rho_{exp} = \tan\Psi \exp(i\Delta)$$

Based on an optical model for the film growth process, to be discussed in detail below, and using the Bruggeman effective medium approximation[18], BEMA, to model multi-component layers, ρ_{cal} is calculated for the model using a literature database for the known constituents of the film and substrate. ρ_{cal} is compared with ρ_{exp}, and as a figure of merit for comparison, an unbiased estimator, δ, is calculated from the relationship[19]:

$$\delta = \left[\frac{1}{N-P-1}\Sigma\left|\rho_{exp}-\rho_{cal}\right|^2\right]^{\frac{1}{2}}$$

where N is the number of wavelengths sampled, and P the number of unknown parameters. A minimizing procedure gives the best fit parameters which are film thicknesses and percents for the constituents at the 90 % confidence level.

Because of the time required to perform SE measurements in our system, we used SWE, at 3.5 eV or 354nm, to perform fast (seconds) measurements in real time. This optical energy was chosen for several reasons. One reason is that both Δ and Ψ are accurately measured for both bare and film covered InP at that energy; and another is that ϵ is relatively insensitive to substrate temperature in the temperature range investigated. Figure 2 shows our measured ϵ data for InP at several temperatures of interest in this study. Near 3.5 eV the interesting convergence of ϵ_2 is seen and while ϵ_1 is not as insensitive to temperature, its excursion is small. For all the semiconductors that we have recently worked with (Si, Ge, InP, InSb) we have observed particular wavelength regions that are appropriate for temperature sensitive and insensitive measurements[20] and we have termed these special wavelengths chosen for specific measurements, "magic wavelengths".

Optical Models. In order to analyze the ellipsometrically measured Δ,Ψ data, optical models that describe the film substrate system are required. The models are deduced from independent measurements of composition and chemical bonding to identify constituents and other relevant parameters such as film thicknesses. In this study we use x-ray photoelectron spectroscopy, XPS, and chemical etching results along with the ellipsometry measurements for model construction.

For the case of thermal oxidation of InP, there are several reports attesting to the

existence of two distinct layers[4,5] with the outermost layer being predominantly In_2O_3 and the inner layer a mixture of $InPO_4$ and with P and perhaps some other oxides. These chemically different layers could be differentiated by different chemical etch rates. Figure 3 shows SE results analyzed using a two film on InP model (discussed below) on the etching of the ECR grown oxide in two different HF/H_2O solutions. The total film thickness is reported. The sharp change in film etch rate strongly indicates a two layer system, as we found previously with the HF etching of InP thermal oxides[5] with the outermost oxide etching relatively fast. Thus we show strong evidence that two distinct layers exist. Similar results were found for electrochemical oxides on InP with two layers after an initial thin oxide[21].

Figure 4a shows a typical XPS survey spectrum after ECR plasma oxidation of InP, but before etching to show the outer layer; this spectrum shows essentially In_2O_3. The Figure 4b survey spectrum taken after etching shows that once the fast etching outer layer is removed, a slow etching predominantly P layer is seen on the InP surface with only small amounts of In and O. Figure 4c is a typical XPS spectrum of the P spectral region. At 134.7 eV the small peak is attributed to oxidized P, and at 129 eV is also a small peak for P in InP. In between the peaks at around 131 eV, are the free P peaks. These results are concordant with literature findings for the thermal oxidation of InP, and lead us to adopt a two layer optical model where the outer layer is assumed to be pure In_2O_3 for simplicity, and the inner layer is a mixture of a-InP and $In(PO_3)_3$. For the inner layer, the dielectric function for a-InP is used in place of that for P, only because there is no dielectric function data available for P, and likewise the dielectric function for $In(PO_3)_3$ is used as the inner

layer oxidized species based on previous work[22] even though we do not characterize the stoichiometry of the inner oxide in this work.

While the two layer model is reasonably justified based on both etching and XPS data, it should be remembered that it is a model based upon incomplete knowledge and available data and the interpretations based upon the use of this model must be treated in this context.

We now attempt to fit the SE data to this developed two layer model and several reasonable alternatives. Figure 5 shows the results of fitting a SE spectrum from ECR grown oxide on InP to five reasonable models, A-E. Substantially the same results were obtained for all biases, temperatures and times of oxidation used in this study. The figure of merit of the fit, δ, is always lowest for two film models, and this agrees with our etch and XPS data above. The two film models have the same outer layer of In_2O_3, since that is in agreement with our XPS data and models D and E compare inner layers of a-InP with $In(PO_3)_3$ or In_2O_3. There exists reports that the innermost layer is either $In(PO_3)_3$[23] from electrochemical oxidation or $InPO_4$ from thermal oxidation[4]. However, since there are no available dielectric functions for $InPO_4$, this possibility has not been tested, but a good fit has been obtained with D and so this model will be used for the analyses that follow. Figure 6 shows the excellent fit of model D (solid line) the experimental data (open circles).

Experimental Results and Discussion

In this section the oxide growth law is deduced from the SE data and modelling, and then SWE real time kinetics results are presented.

Figure 7 shows a representative set of SE spectra for the time evolution of ECR plasma oxidation of InP under one set of conditions. This kind of SE data was analyzed according to model D to yield thicknesses for both the top In_2O_3 film and the mixed composition interface layer. Figure 8 a-c displays representative SE data taken under different growth conditions, and analyzed by model D in terms of the thicknesses of the two layers. A comparison of these results indicates that the positive substrate biases (Figure 8b) enhance the growth of both layers while zero bias (Figure 8a) slightly retards the growth of the interface layer. With negative bias Figure 8c shows evidence for etching with both outer and inner layers being affected. However, the etching behavior is more complex than simply ion etching. Figure 9 shows the etching effects more clearly with a larger negative bias where at first the top layer is etched, then after about 2 min both layers are etched. Simultaneous with etching the ion bombardment also damages the oxide, and thus may alter the dielectric functions causing the apparent abrupt changes in etching behavior. Etching at negative bias was also reported[24] for ECR plasma oxidation in the Si and Ge systems.

Figure 10 shows the total thickness versus $t^{1/2}$ as obtained from SE measurements. It is seen that the oxide growth is enhanced by both higher substrate temperature and positive bias. Positive bias substantially affects the rate of oxidation after an initial regime (of about 10nm for 250°C) indicating the onset of diffusion control. Diffusion control is evidenced by linearity of the plot after an initial regime that is nearly bias independent but temperature dependent. The negative bias condition shows limited growth indicative of initially only growth, but then growth balanced by etching.

Figure 11 shows SWE real time Δ,Ψ ellipsometry data at three different biases. In the early stage of exposure of InP to the O plasma, starting from the upper left in the Figure one trajectory is followed by all the bias conditions, indicating film growth, viz. decreasing Δ and increasing Ψ, with the same film optical properties. Of course as shown above, the rate of growth is a function of bias and temperature. (The experiments were done with no applied substrate heating. The substrate heating observed was measured and the result of electron and/or ion bombardment from the plasma) The zero bias trajectory with substrate temperature of 120°C ceases to grow beyond a total film thickness of 9.4nm. This is similar to InP thermal oxidation results which show considerable thermal activation hence temperature sensitivity. The negative and positive bias trajectories continue towards lower Δ, but for the negative bias condition growth ceases with a decreasing Ψ (to the left in the Figure) which is indicative of a different phenomena than growth or etching. This is corroborated by the SE results in Figure 8c and 9 for negative biases where it is likely that etching with damage is occurring simultaneous with growth. When growth ceases the continual bombardment by positive plasma species causes damage as evidenced by an increase in the apparent complex refractive index which would decrease Ψ, as is observed. For positive bias, continual film growth is evidenced by the monotonic decrease in Δ and increase in Ψ to a thickness of about 35nm. Figure 12 shows the positive bias data from Figure 11 along with simulations made using a two layer film growth model where the ratio of the layer thicknesses, inner layer/outer layer, L_{in}/L_{out}, is varied from 0.1 to 10. It is seen that for the ratio of one, the positive bias data is closely approximated and this is also corroborated in Figure 8b. As seen in Figure 12, a ratio less than one is above the data

while greater than one is below. Thus, both layers grow together with positive bias.

In view of both the present ECR InP studies and our past results on Si and Ge there is a strong resemblance of ECR plasma oxidation to thermal oxidation kinetics. This is likely the result of the low electric field across the oxide for ECR oxidation. The larger part of the potential drop is across the plasma sheath rather than across the growing oxide. The 0V bias results show a saturation thickness that is temperature dependent. The thermal oxidation of InP as well as ECR oxidation creates an excess of P at the interface which is indicated using the two layer model as growth of the interface or inner P rich layer (simulated using a-InP in Model D). This fact renders both oxidation techniques useless for the production of InP MOS devices where low surface electronic states is important. Different from thermal oxidation is the observation for ECR oxidation that at any temperature and after an initial growth regime the bias effects both layers indicating that at least one of the kinetically important oxidation species is charged.

Acknowledgements

This research was supported in part by the Office of Naval Research, ONR, and the National Science Foundation, NSF.

List of Figures

Table I Calculation results from SE data of Fig.1 for InP surface cleaning using a one layer model, in comparison with AFM results.

Sample/Treatment	Composition		Thickness (nm)	$\delta x10^4$	AFM RMS (nm)
	a-InP	$In(PO_3)_3$			
X / Cleaned	61%	39%	0.47±0.14	54	0.25
Y / Cleaned	66%	34%	0.98±0.15	58	0.51
X / Degreased Only	56%	44%	1.59±0.15	56	0.27

1. E.A. Irene, CRC Critical Reviews in Solid State and Materials Science, Ed. J.E. Greene, Vol 14(2), pp 175-223 (1988).

2. L.G. Meiners and H.H. Wieder, Materials Sci. Reports, 3, 139 (1988).

3. G. Hollinger, J. Joseph, Y. Robach, E. Bergignat, B. Commerce, P. Viktorovitch and M. Froment, J. Vac. Sci. Technol. B, 5, 1108 (1987).

4. A. Nelson, K. Geib and C.W. Wilmsen, J. Appl. Phys., 54, 4134 (1983).

5. X. Liu, M.S. Denker and E.A. Irene, J. Electrochem. Soc., 139, 799 (1992).

6. Y.Z. Hu, M. Li, Y. Wang, E.A. Irene, M. Rowe and H.C. Casey Jr., Appl. Phys. Lett., submitted for publication (1993).

7. D.A. Carl, D.W. Hess, M.A. Lieberman, T.S. Nguyen and R. Gronsky, J. Appl. Phys. 70, 3301 (1991).

8. Y.Z. Hu, J. Joseph and E.A. Irene, Appl. Phys. Lett. 59, 1353(1991).

9. J. Joseph, Y.Z. Hu and E.A. Irene, J. Vac. Sci. Technol. B, 10, 611 (1992).

10. J. Joseph, Y.Z. Hu and E.A. Irene, Proceedings of ECS St. Louis (1992).

11. J. Andrews, Y.Z. Hu and E.A. Irene, SPIE Proc., 1188, 162 (1990).

12. A.A. Shatas, Y.Z. Hu and E.A. Irene, J. Vac. Sci. and Tech. A, 10, 3119 (1992).

13. X. Liu, J.W. Andrews and E.A. Irene, J. Electrochem. Soc., 138, 1106 (1991).

14. F.N. Schwettman, K.L. Chiang and W.A. Brown, Abstract 276 p688, The Electrochem. Soc. Extended Abstracts, Vol 78-1, Seattle WA, May 21-26, 1978.

15. G. Gould and E.A. Irene, J. Electrochem. Soc.,134, 1031 (1987).

16. D.E. Aspnes, in B.O. Seraphin (ed.) "Optical Properties of Solids: New Developments", North Holland, 1976, p799.

17. D.E. Aspnes and A.A. Studna, Phys. Rev. B, 27, 985 (1983).

18. D.A.G. Bruggeman, Ann. Phys. (Leipzig), 24, 636 (1935).

19. D.E. Aspnes, J.B. Theeten and F. Hottier, Phys. Rev. B20,3992(1979).

20. E.A. Irene, presented at the First International Conference on Spectroscopic Ellipsometry, Paris, France, Jan. 11-14, 1993 and accepted for publication in Thin Solid Films.

21. M.P. Bresland, Y. Robach and J. Joseph, J. Electrochem. Soc., 140, 1 (1993).

22. Y. Robach, A. Gagnaire, J. Joseph, E. Bergignat and G. Hollinger, Thin Solid Films, 162, 81 (1988).

23. Y. Robach, J. Joseph, G. Hollinger and P. Viktorovitch, Appl. Phys. Lett., 49, 1281 (1986).

24. Y.Z. Hu, J. Joseph and E.A. Irene, presented at 39th American Vacuum Soc. Meeting, Chicago IL, Nov. 7-13 1992, accepted for publication J. Vac. Sci. Technol. A, 1993.

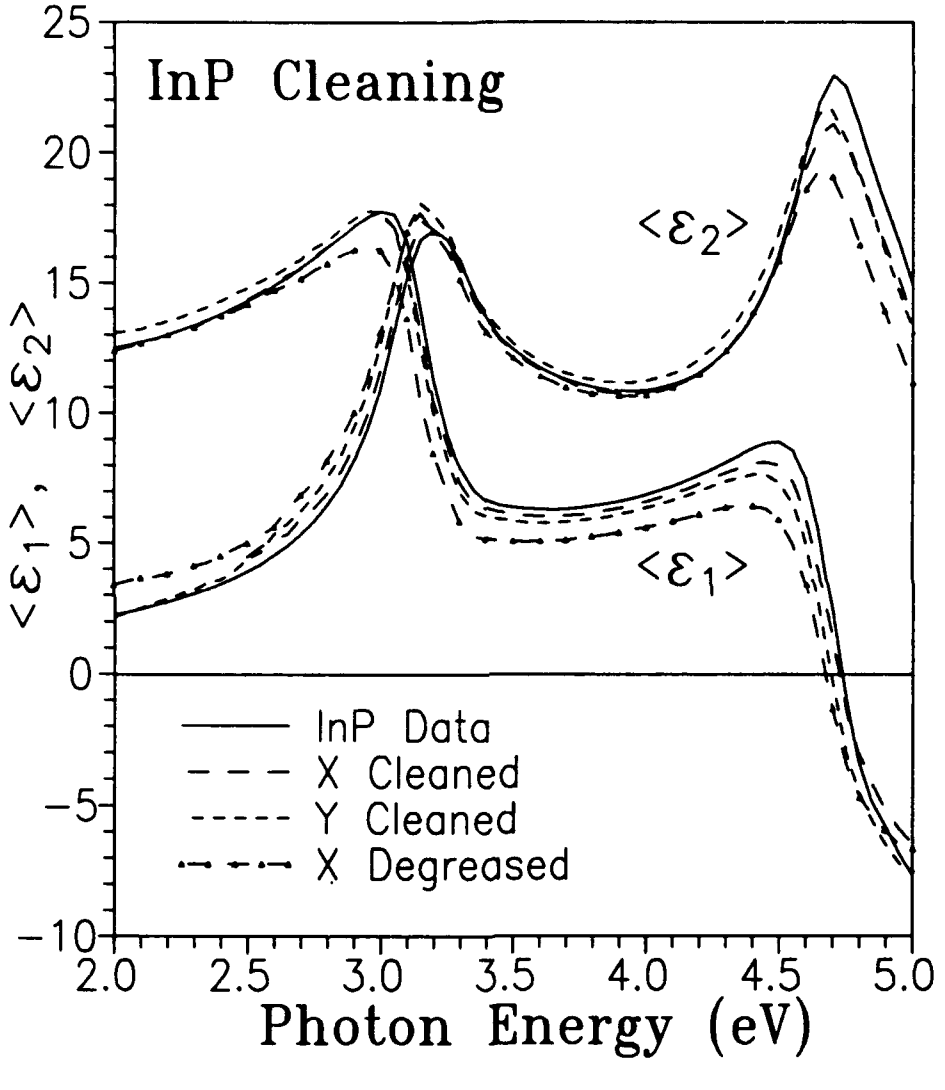
InP Cleaning
$\langle\varepsilon_2\rangle$
$\langle\varepsilon_1\rangle$
$\langle\varepsilon_1\rangle$, $\langle\varepsilon_2\rangle$
InP Data
X Cleaned
Y Cleaned
X Degreased
Photon Energy (eV)
25
20
15
10
5
0
−5
−10
2.0
2.5
3.0
3.5
4.0
4.5
5.0

Fig. 1.

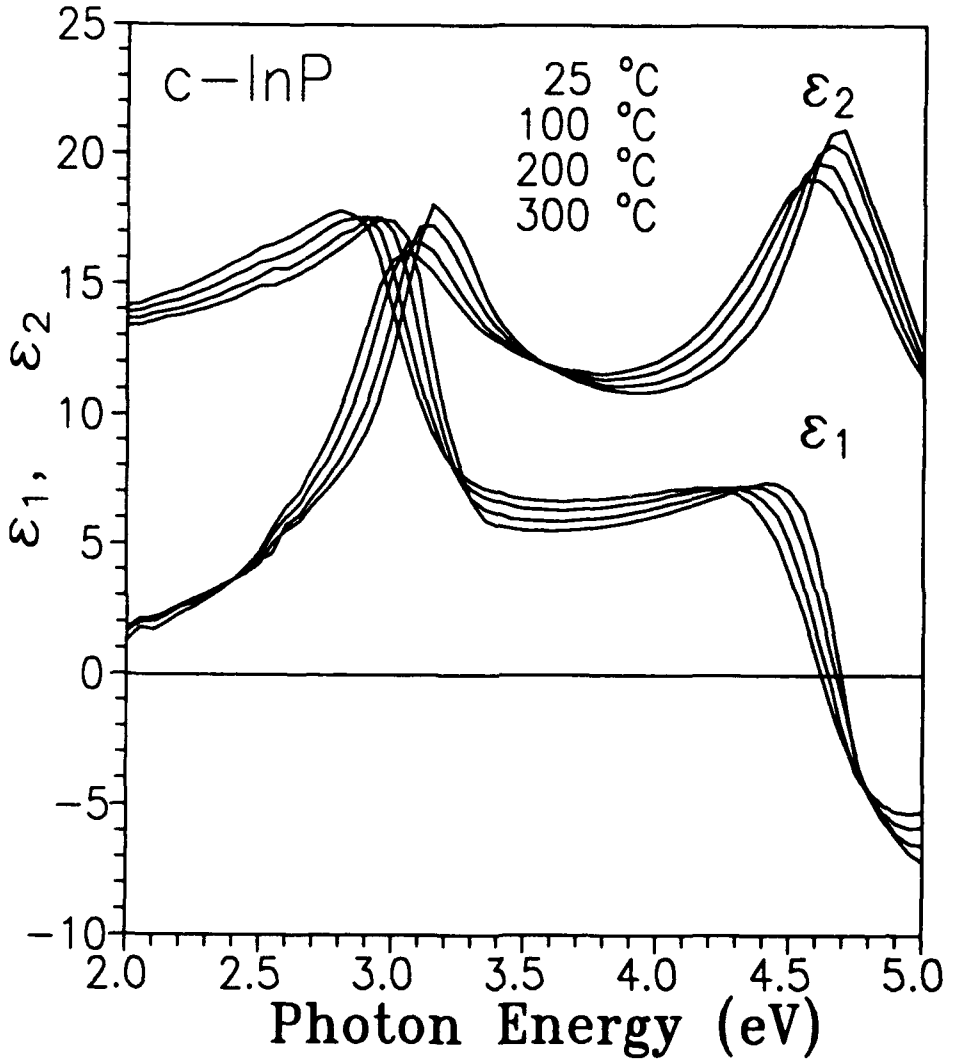
c–InP
25 °C
100 °C
200 °C
300 °C
ε2
ε1
ε1, ε2
25
20
15
10
5
0
−5
−10
2.0
2.5
3.0
3.5
4.0
4.5
5.0
Photon Energy (eV)

Fig. 2

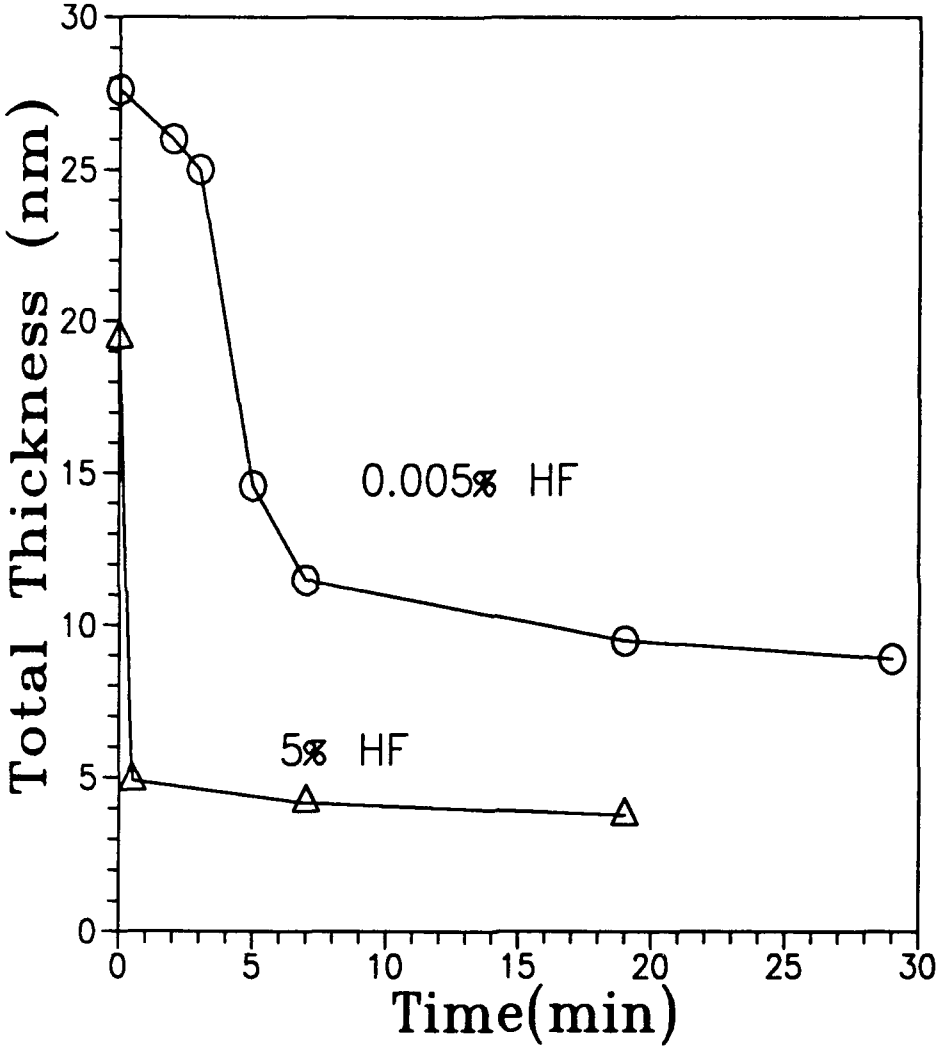
Total Thickness (nm)
30
25
20
15
10
5
0
0.005% HF
5% HF
0
5
10
15
20
25
30
Time(min)

Fig 3

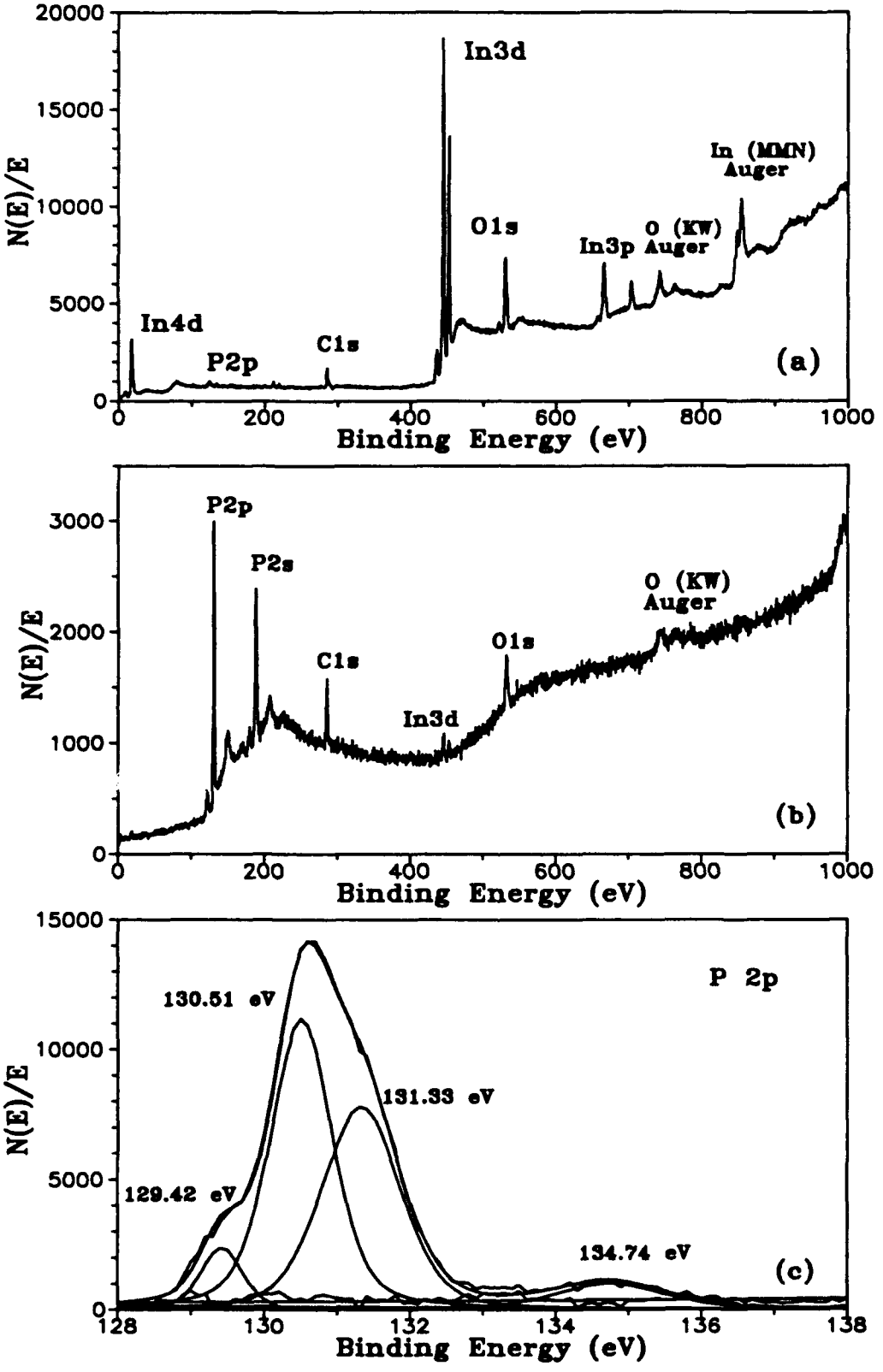
20000
15000
10000
5000
0
N(E)/E
In3d
In (MMN) Auger
O1s
O (KW) Auger
In3p
In4d
P2p
C1s
(a)
0
200
400
600
800
1000
Binding Energy (eV)
3000
2000
1000
P2p
P2s
O (KW) Auger
C1s
O1s
In3d
(b)
15000
10000
5000
P 2p
130.51 eV
131.33 eV
129.42 eV
134.74 eV
(c)
128
130
132
134
136
138

Fig 4

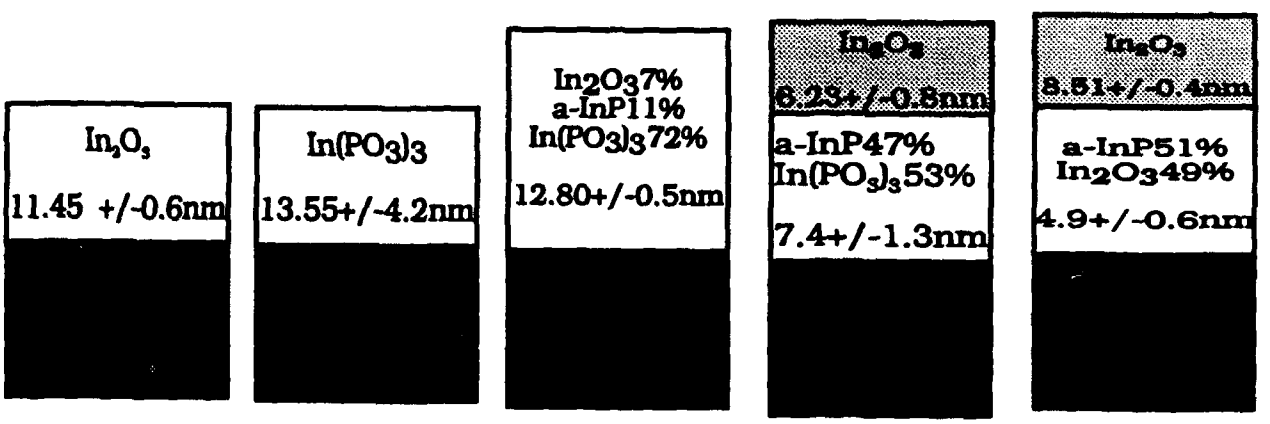

$\delta = 0.0155$ $\delta = 0.0752$ $\delta = 0.0182$ $\delta = 0.0037$ $\delta = 0.0062$

A **B** **C** **D** **E**

Fig 5

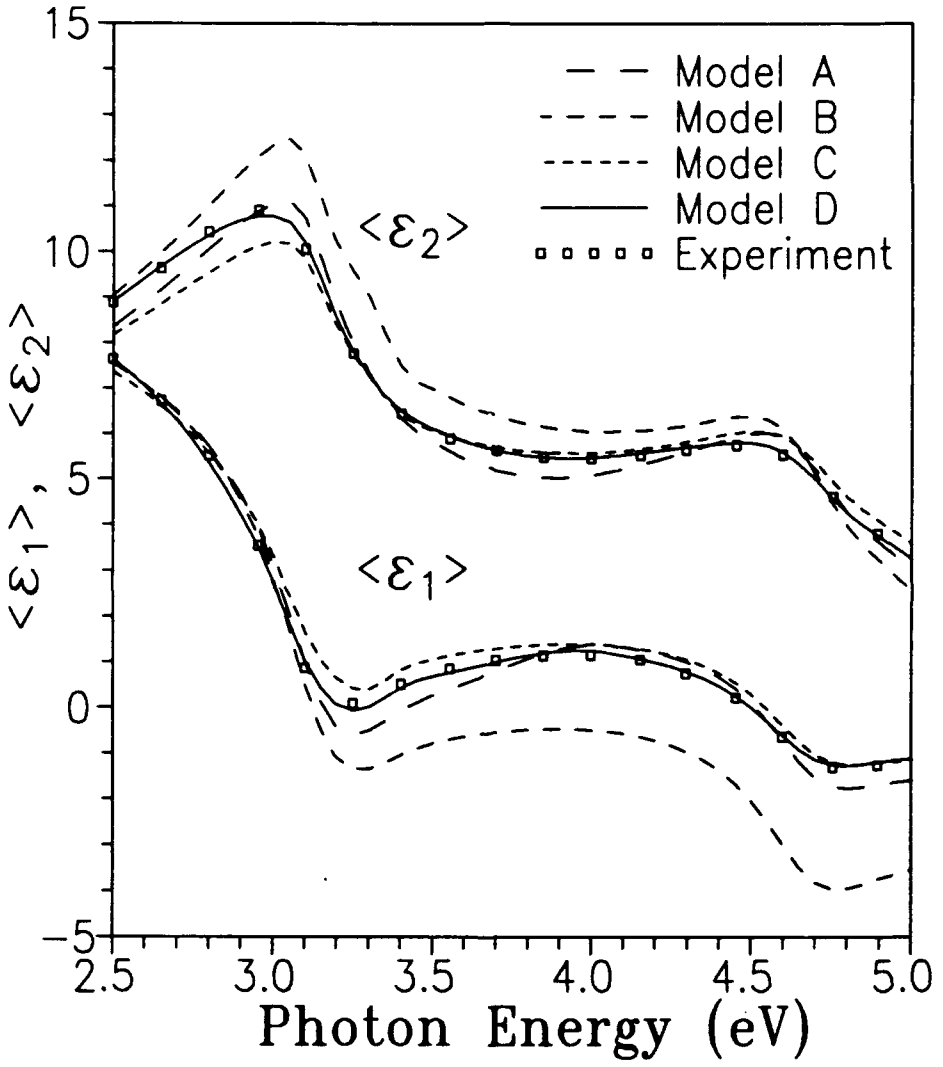
15
10
5
0
−5
2.5
3.0
3.5
4.0
4.5
5.0
Photon Energy (eV)
<ε1>, <ε2>
<ε2>
<ε1>
Model A
Model B
Model C
Model D
Experiment

Fig 6

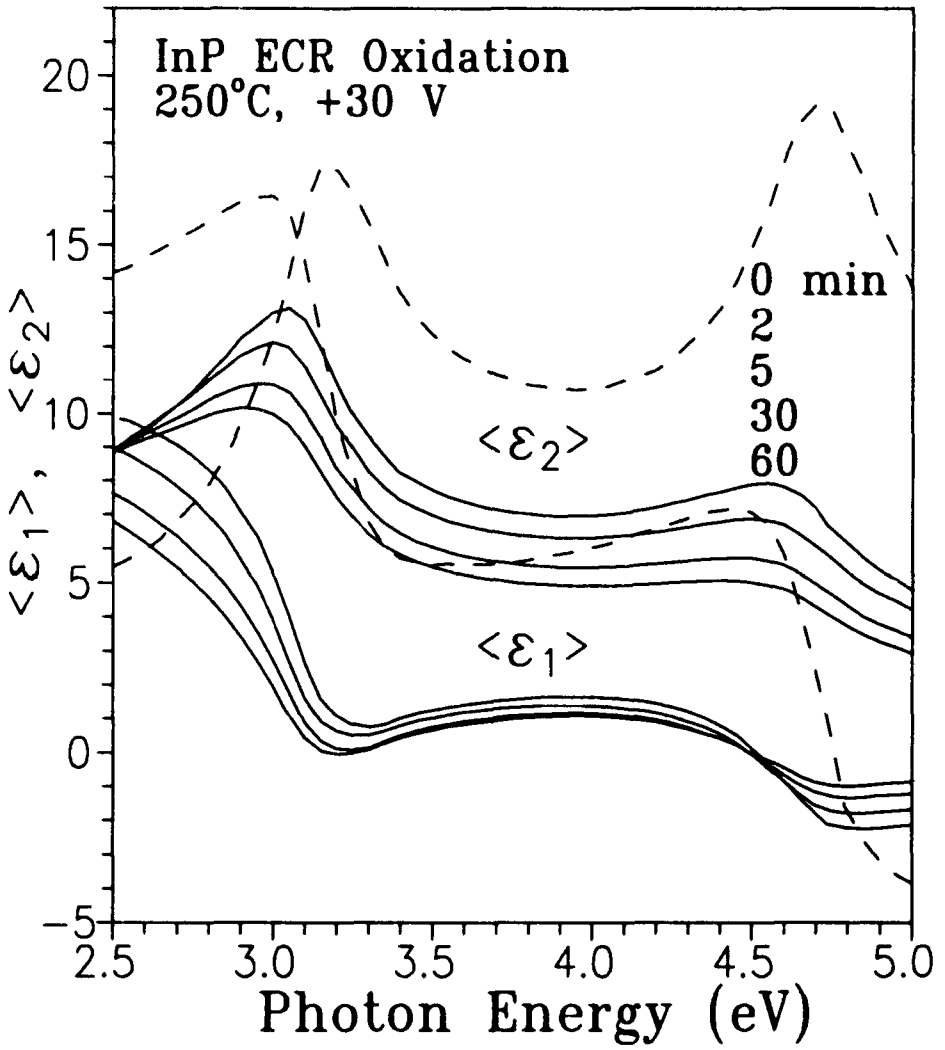
InP ECR Oxidation
250°C, +30 V
0 min
2
5
30
60
<ε2>
<ε1>
<ε1>, <ε2>
Photon Energy (eV)
20
15
10
5
0
−5
2.5
3.0
3.5
4.0
4.5
5.0

F.9.7

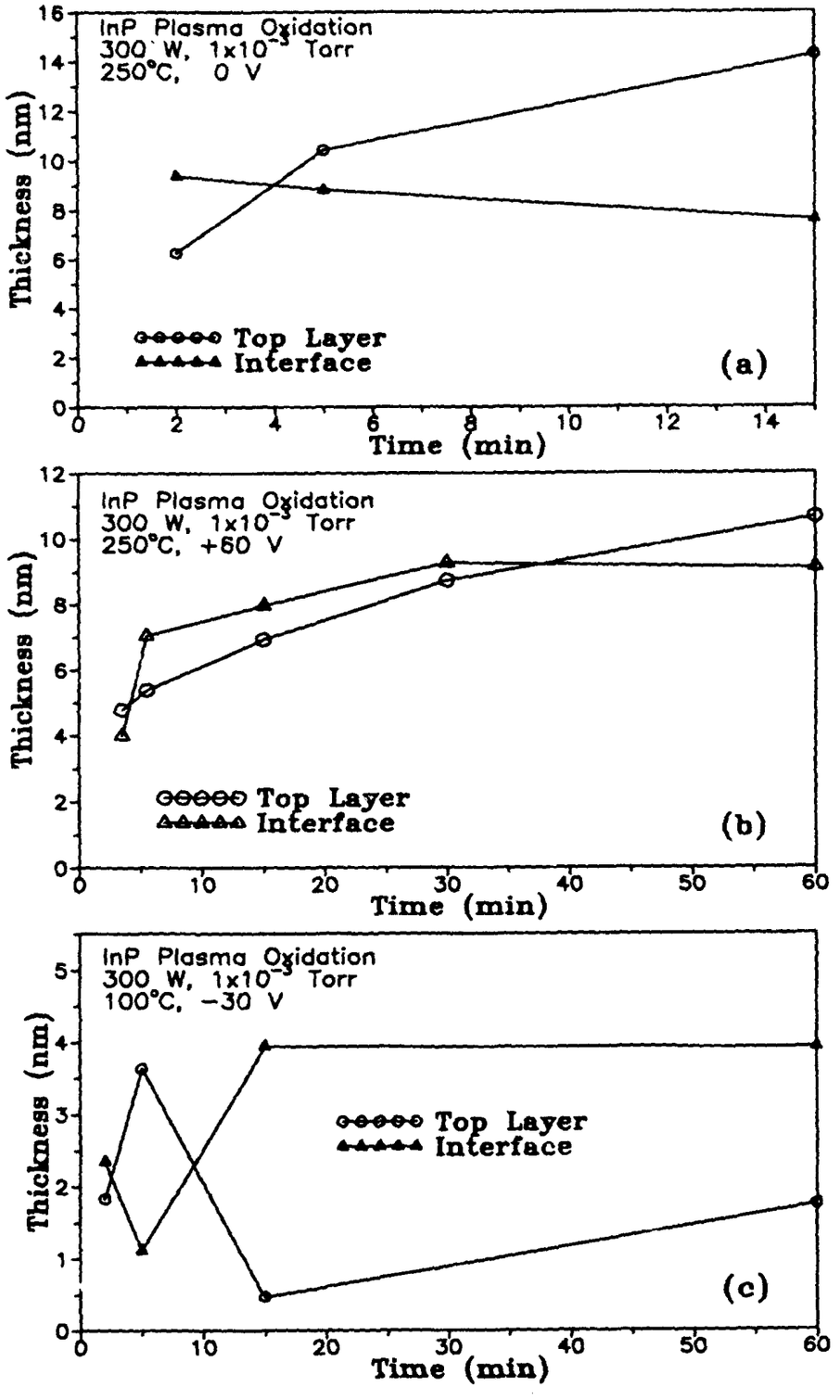
InP Plasma Oxidation
300 W, 1x10⁻³ Torr
250°C, 0 V
Thickness (nm)
Time (min)
Top Layer
Interface
(a)
InP Plasma Oxidation
300 W, 1x10⁻³ Torr
250°C, +60 V
Thickness (nm)
Time (min)
Top Layer
Interface
(b)
InP Plasma Oxidation
300 W, 1x10⁻³ Torr
100°C, −30 V
Thickness (nm)
Time (min)
Top Layer
Interface
(c)

Fig 2

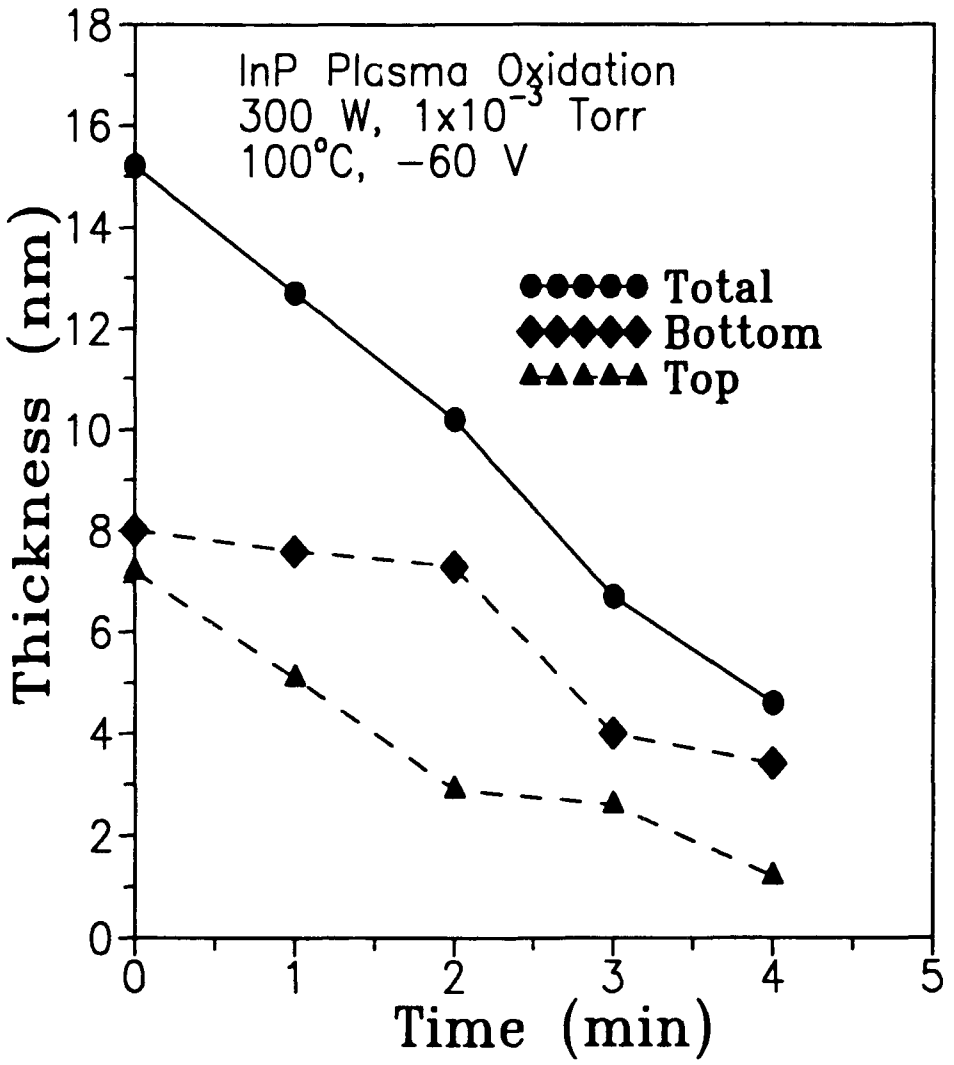
InP Plasma Oxidation
300 W, 1x10^{-3} Torr
100°C, −60 V
Total
Bottom
Top
Thickness (nm)
Time (min)
0
2
4
6
8
10
12
14
16
18
0
1
2
3
4
5

Fig 9

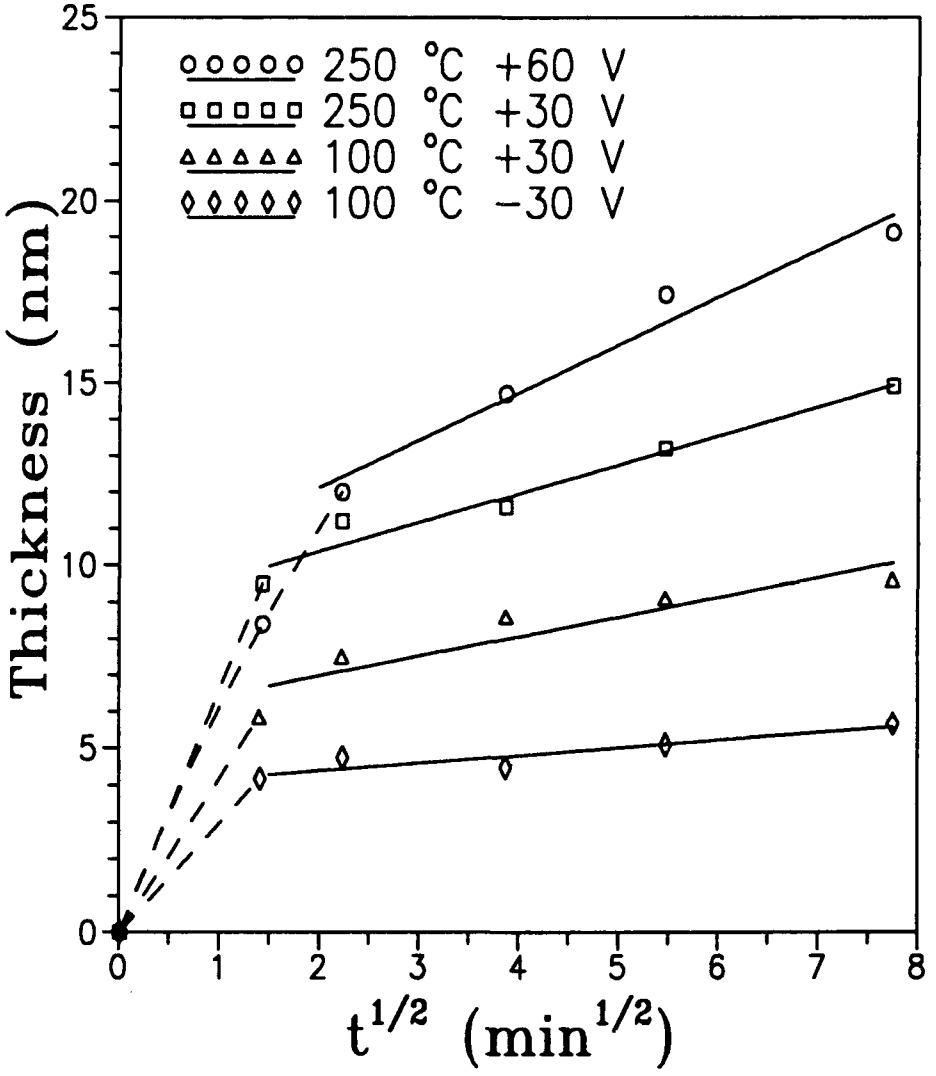
250 °C +60 V
250 °C +30 V
100 °C +30 V
100 °C −30 V
Thickness (nm)
t^1/2 (min^1/2)
0
5
10
15
20
25
0
1
2
3
4
5
6
7
8

Fig

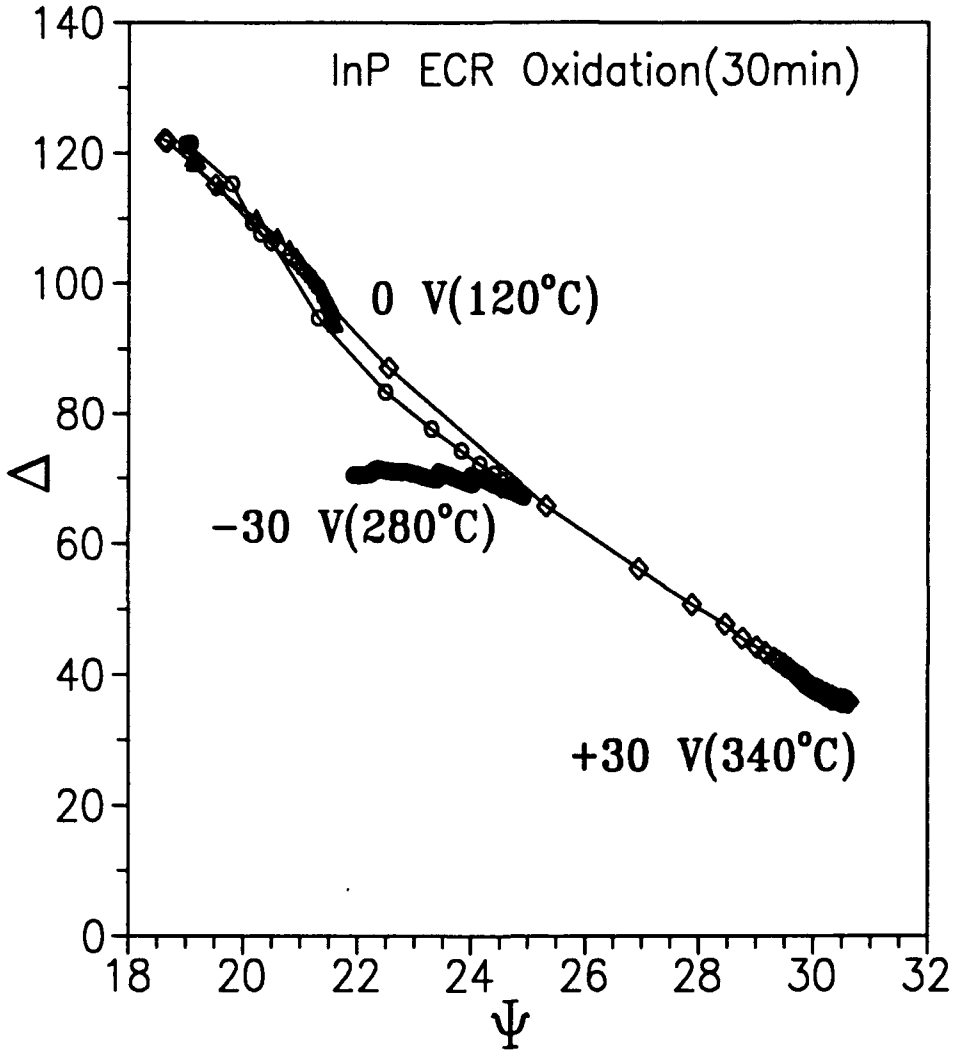
InP ECR Oxidation(30min)
0 V(120°C)
−30 V(280°C)
+30 V(340°C)
Δ
Ψ
140
120
100
80
60
40
20
0
18
20
22
24
26
28
30
32

Fig 11

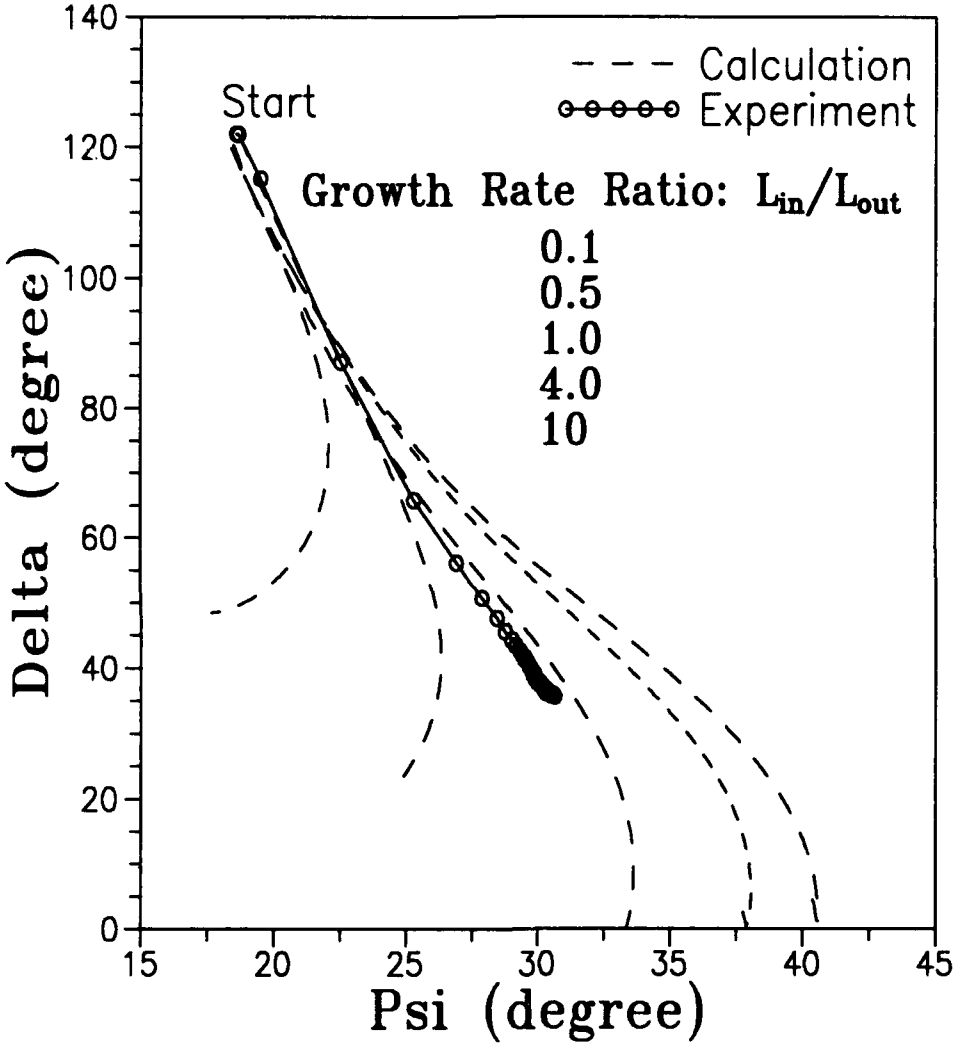
Start
Calculation
Experiment
Growth Rate Ratio: L_{in}/L_{out}
0.1
0.5
1.0
4.0
10
Delta (degree)
Psi (degree)
140
120
100
80
60
40
20
0
15
20
25
30
35
40
45

Fig 12